ELSEVIER

International Journal of Heat and Fluid Flow 21 (2000) 520–525

International Journal of
HEAT AND
FLUID FLOW

www.elsevier.com/locate/ijhff

Characteristics of turbulent combined-convection boundary layer along a vertical heated plate

Yasuo Hattori [a,*], Toshihiro Tsuji [b], Yasutaka Nagano [c], Nobukazu Tanaka [a]

[a] *Hydraulics Department, Central Research Institute of Electric Power Industry, 1646 Abiko, Abiko-shi, Chiba-ken 270-1194, Japan*
[b] *Department of Mechanical Engineering, Nagoya Institute of Technology, Gokiso-cho, Showa-ku, Nagoya 466-8555, Japan*
[c] *Department of Environmental Technology, Graduate School of Engineering, Nagoya Institute of Technology, Nagoya, Japan*

Abstract

Fluid flow and heat transfer characteristics in a turbulent combined-convection boundary layer in air along a vertical heated plate have been investigated with normal hot and cold wires. The measured heat transfer rates and turbulent quantities show that the turbulent transition moves downstream with a slight increase in freestream velocity. Then, the heat transfer rate rapidly decreases to about 40% of that obtained in the turbulent natural-convection boundary layer, and velocity and temperature fluctuations become smaller in amplitude and change from random to harmonic at a specific frequency. Thus, the characteristics of the turbulent combined-convection boundary layer differ in several respects from those observed in both natural and forced convections. Based on the experimental results, the regimes of boundary layer flows are classified as a function of local Reynolds and Grashof numbers.

Keywords: Combined convection; Turbulent flow; Convective heat transfer; Boundary layer; How-wire measurement

1. Introduction

In designing electric power plants, it is indispensable to correctly evaluate the heat transfer characteristics of turbulent combined-convection boundary layers (Hattori et al., 1995). Combined-convection phenomena are frequently encountered in both nature and engineering applications, and many studies have been reported. However, most of them are concerned with laminar combined-convection flows, and there are few investigations on turbulent combined convection. Therefore, the turbulent characteristics of combined convection have yet to be clarified, and the accumulation of experimental data for turbulent quantities is eagerly awaited.

The turbulent natural-convection boundary layer aided by a freestream along a vertical heated plate is one of the typical turbulent combined-convection flows. For this boundary layer flow, it has been determined that turbulence is suppressed and the heat transfer rate decreased under certain conditions (Hall and Price, 1970).

Kitamura and Inagaki (1987) and Inagaki and Kitamura (1988) conducted experiments with water and air as the working fluid and obtained the quantitative correlation between the heat transfer rate and flow conditions. In their experiment with water (Kitamura and Inagaki, 1987), the changes in the velocity and temperature fields were also investigated by using a hot-film probe and a flow visualization technique. However, the origin of the reduction in heat transfer rate has not been clearly traced because reliable measurements of turbulent quantities near the wall are very difficult for low-speed flows with relatively large fluctuations in velocity and temperature. Krishnamurthy and Gebhart (1989) also performed measurements on a combined-convection boundary layer flow of compressed air. They indicated that the turbulent transition of the boundary layer was delayed with increasing freestream velocity, but their study focused on the transition from laminar to turbulence in combined convection.

Recently, Patel et al. (1998) numerically examined the heat transfer characteristics from turbulent natural convection to turbulent forced convection along a vertical plate by using a low Reynolds-number turbulence model. They predicted the reduction in heat transfer rate in the combined-convection region and proposed a map of the various convection flow regimes classified based on a criterion for the variation in heat transfer rate. However, the capability of the turbulence model was not verified because of the conclusive lack of experimental data for turbulent quantities in combined convection.

The purpose of this study is to clarify how the fluid flow and heat transfer characteristics in the turbulent natural-convection boundary layer change with the introduction of freestream velocity and to accumulate credible experimental data for turbulent combined convection. Measurement with normal hot and cold wires has been mainly conducted in the near-wall region of the combined-convection boundary layer in air. The

* Corresponding author. Tel.: +81-471-82-1181; fax: +81-471-84-7142.
E-mail address: yhattori@criepi.denken.or.jp (Y. Hattori).

0142-727X/00/$ - see front matter
PII: S0142-727X(00)00040-0

Notation

E_u, E_t	spectrum functions of velocity fluctuations u and t
f	frequency
Grx	local Grashof number, $Grx = g\beta\Delta T_w x^3/v^2$
g	gravitational acceleration
h	heat transfer coefficient
Nux	local Nusselt number, $Nux = hx/\lambda$
Rex	local Reynolds number, $Rex = U_\infty x/v$
Rix	local Richardson number, $Rix = Grx/Rex^2$
T	mean fluid temperature
t	temperature fluctuation
U	mean streamwise velocity
U_m	maximum velocity along the flat plate
u	streamwise velocity fluctuation
x	distance from the leading edge of the flat plate
y	distance perpendicular to the flat plate

Greeks

β	coefficient of volume expansion
λ	thermal conductivity
v	kinematic viscosity

Superscripts and subscripts

$\bar{(\ )}$	time-averaged quantities
w	wall condition
∞	ambient condition

variations in mean and turbulent quantities in the velocity and thermal fields with increasing freestream velocity are discussed, especially paying attention to the effect of a slight freestream on turbulent natural convection. Then, the regimes of various boundary layer flows are identified based on the turbulent characteristics.

2. Experimental apparatus and procedure

Fig. 1 shows a schematic drawing of experimental apparatus, which consists of a vertical wind tunnel, heaters and measurement instruments. The heated surface generating flow was an aluminum plate 4 m high, 0.8 m wide and 0.02 m thick. The surface was finished to a smooth mirror for preventing heat loss by radiation. Twenty electric heaters were attached to the back of the plate, and the surface temperature was kept uniform by controlling the heating current of each.

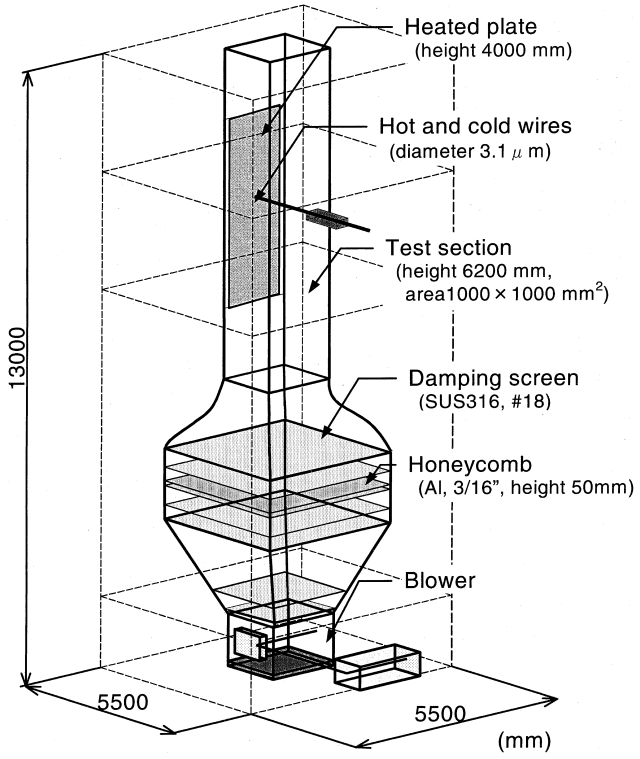

Fig. 1. Schematic drawing of experimental apparatus.

The vertical wind tunnel with solid boundary was designed in accordance with previous reports (Fukatsu, 1934; Lumley, 1964; Rae and Pope, 1984) to produce an ideal flow field. The heated plate was placed vertically in the test section 1×1 m^2 in area and 6.2 m high. The maximum power of a motor-driven blower was 11 kW, and a freestream velocity U_∞ up to about 10 m/s was obtained in the test section. In the settling chamber 2×2 m^2 in area and 1 m long, four damping screens and a honeycomb were installed. With this experimental apparatus, the turbulent boundary layer in both natural and forced convections along a vertical heated plate could be developed.

Instantaneous velocity and temperature were measured with normal hot and cold wires made of 3.1 μm diameter tungsten. The sensitive length of the hot and cold wires was 2 and 4 mm, respectively, and the cold wire was located 2.5 mm upstream of the hot wire. Temperature compensation of the hot wire was carried out by the technique of Hishida and Nagano (1978). The measurement error caused by the spatial difference between the wires was minimized by delaying temperature signals of the cold wire with Taylor's hypothesis. The amplified voltage outputs of these wires were processed with a personal computer after analog to digital conversion.

The thermal and flow conditions in the test section and the accuracy of measurements were verified in the preliminary experiments. The uniformity of surface temperature was within 0.5°C, and the spatial non-uniformity ratio and the relative fluctuation ratio of freestream velocity were below 1.6% and 0.8%, respectively. It was confirmed that turbulent quantities measured near the wall in the natural-convection boundary layer agreed well with the data taken by Tsuji and Nagano (1988).

Experiments were carried out under the conditions of uniform surface temperature T_w in the range of 40–100°C. The ambient fluid temperature T_∞ was somewhat different for each experiment within 23–29°C. The vertical distance x from the leading edge of the flat plate to the measuring locations changed from 0.265 to 3.765 m. The ranges of local Reynolds number $Re\,x$ and local Grashof number $Gr\,x$ were 0–1.9×10^6 and 1.3×10^8–3.5×10^{11}, respectively. Physical properties were evaluated at the film temperature $T_f = (T_w + T_\infty)/2$ except for β.

3. Results and discussion

3.1. Local heat transfer rate

Heat transfer characteristics of the turbulent natural-convection boundary layer with the introduction of freestream velocity were investigated. The heat transfer rates were

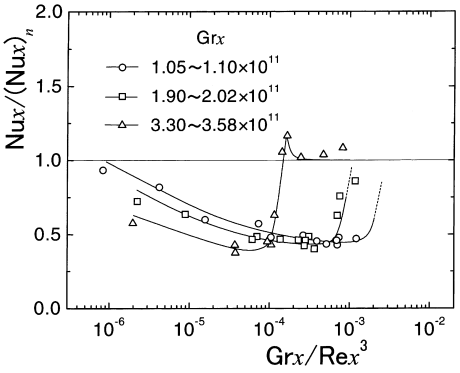

Fig. 2. Local heat transfer rate.

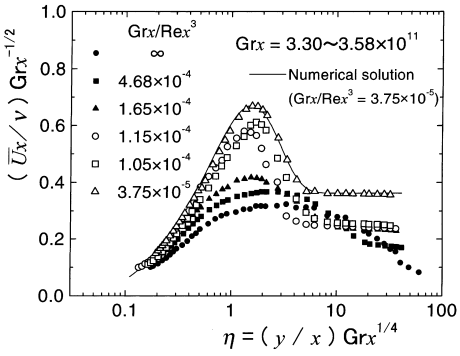

Fig. 3. Mean velocity profile.

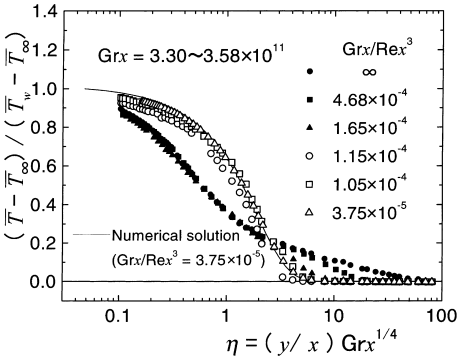

Fig. 4. Mean temperature profile.

estimated from temperature gradients near the wall. For various Grashof numbers, local Nusselt numbers $Nu\,x$ are shown in Fig. 2. The value of $Nu\,x$ is normalized with that of turbulent pure natural convection $(Nu\,x)_n$, and $Gr\,x/Re\,x^3$ is taken as the coordinate. For constant $Gr\,x$, a decrease in $Gr\,x/Re\,x^3$ implies an increase in freestream velocity. On the other hand, if $Gr\,x/Re\,x^3$ and the thermal condition are constant, a change in $Gr\,x$ corresponds to that in x.

A drastic reduction in $Nu\,x$ with increasing freestream velocity is observed, i.e., $Nu\,x/(Nu\,x)_n$ decreases to about 0.4 at a value of $Gr\,x/Re\,x^3$ for a given $Gr\,x$. When attention is paid to $Grx/Rex^3 \simeq 10^{-3}$, $Nu\,x/(Nu\,x)_n$ decreases with decreasing $Gr\,x$ and takes the smallest value at $Grx = 1.05 \times 10^{11}$–$1.10 \times 10^{11}$. This signifies that $Nu\,x$ still remains at a high value in the region downstream of the location, where the $Nu\,x$ reduction occurs with increasing freestream velocity.

A decrease in $Nu\,x$ with increasing freestream velocity in the combined-convection boundary layer is also observed in the experiment with air of Inagaki and Kitamura (1988). In their experiment, however, the minimum value of $Nu\,x/(Nu\,x)_n$ remained at about 0.75, and the occurrence of $Nu\,x$ reduction was not so abrupt as that in the present experiment. The discrepancy between both results may be attributed to differences in the experimental setup and conditions. In their experiment, a test section with a small area was used and relatively large disturbances were involved in the freestream, which yielded a transition Reynolds number of a remarkably small value for pure forced convection. We made an effort to control freestream disturbances, and thus it is considered that the essential characteristics of the turbulent combined-convection boundary layer appeared more clearly.

3.2. Mean velocity and mean temperature profiles

The changes in the streamwise mean velocity and mean temperature profiles in the boundary layer for $Grx = 3.30 \times 10^{11}$–$3.58 \times 10^{11}$ and $Grx/Rex^3 = \infty$–3.75×10^{-5} (corresponding to the freestream velocity of 0–1.1 m/s) are shown in Figs. 3 and 4, respectively. The mean velocity U, the mean temperature T and the distance from the wall y are normalized as the similarity variables used for the laminar natural-convection boundary layer. Since $Gr\,x$ and x are almost constant, the abscissa $\eta(=(y/x)Grx^{1/4})$ is directly proportional to the distance from the wall. As seen in these figures, the mean velocity and temperature profiles markedly change with the introduction of freestream velocity. With increasing freestream velocity, the thicknesses of velocity and thermal boundary layers decrease, and the maximum mean velocity increases and its location approaches the wall. At $Grx/Rex^3 = 1.65 \times 10^{-4}$, the dimensionless value of the maximum mean velocity which is 0.41 at $Grx/Rex^3 = 1.15 \times 10^{-4}$ reaches 0.58 with a slight increase in freestream velocity, at which point the sudden decrease in local heat transfer rate occurs as shown in Fig. 2. Thus, the change in $Nu\,x$ is closely related with those in the mean velocity and mean temperature.

For $Grx/Rex^3 = 3.75 \times 10^{-5}$, the laminar combined-convection boundary layer was calculated numerically, and the profiles of velocity and temperature are plotted by solid lines in Figs. 3 and 4, respectively. The measurements conform well to the calculated results for the laminar boundary layer. Judging from the behavior of turbulent quantities to be discussed below, it is concluded that the combined-convection boundary layer changes from turbulence to laminar with a slight increase in freestream velocity, and that the location of transition to the turbulent boundary layer shifts further downstream.

Krishnamurthy and Gebhart (1989) reported that the transition to turbulence in the combined-convection boundary layer was fairly delayed in comparison with that in pure natural convection. Therefore, such a laminarization of the combined-convection boundary layer may be regarded as a phenomenon caused by the delay of transition.

3.3. Intensities of velocity and temperature fluctuations and turbulent heat flux

Fig. 5 shows the intensity profiles of streamwise velocity fluctuation u normalized by the maximum mean velocity U_m in the transition from turbulence to laminar. In the turbulent natural-convection boundary layer, the maximum intensity of velocity fluctuation occurs at the location $\eta \simeq 25$ beyond the maximum mean velocity location $\eta \simeq 3$. This intensity profile is peculiar to the turbulent natural-convection boundary layer (Tsuji and Nagano, 1988). With the addition of freestream

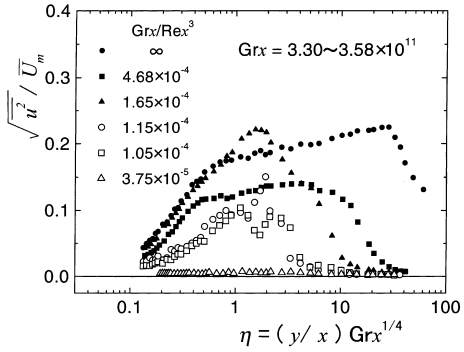

Fig. 5. Intensity of velocity fluctuation.

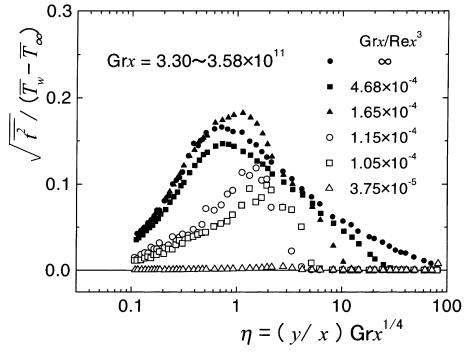

Fig. 6. Intensity of temperature fluctuation.

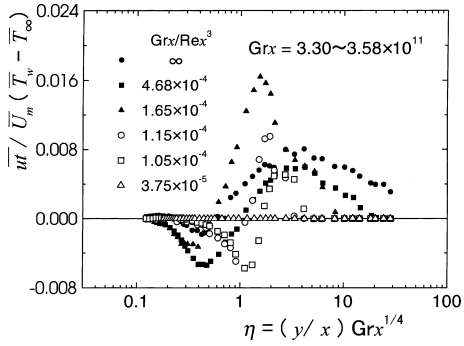

Fig. 7. Turbulent heat flux.

velocity ($Grx/Rex^3 = 4.68 \times 10^{-4}$), the intensity of velocity fluctuation begins to decrease in the whole boundary layer region, although the profile is similar to that in the natural-convection boundary layer.

In the range of $Grx/Rex^3 = 1.65 \times 10^{-4}$–$1.05 \times 10^{-4}$, the intensity profile varies remarkably in accordance with the changes in the local heat transfer rate and mean velocity profile as mentioned previously. At $Grx/Rex^3 = 1.65 \times 10^{-4}$, a fluctuation intensity larger than that in pure natural convection appears at the maximum mean velocity location ($\eta \simeq 1.5$). Moreover, at $Grx/Rex^3 = 1.15 \times 10^{-4}$ and 1.05×10^{-4}, the intensity profile of velocity fluctuation decreases and takes two peaks with an infinitesimal value near the maximum mean velocity location. The occurrence of such a two-peak profile was also observed for different Grx values. In the initial phase of the transition in combined convection, it is confirmed by the linear instability analysis of Carey and Gebhart (1983) and the experiment of Krishnamurthy and Gebhart (1989) that the intensity of velocity fluctuation takes two peaks with an infinitesimal value at the maximum mean velocity location. Therefore, the appearance of the fluctuation intensity profile having two peaks clearly characterizes the transition of the combined-convection boundary layer.

With a further increase in freestream velocity ($Grx/Rex^3 = 3.75 \times 10^{-5}$), the intensity of velocity fluctuation becomes extremely small with the laminarization of the boundary layer. As the freestream velocity becomes sufficiently large ($Grx/Rex^3 < 10^{-6}$), the boundary layer changes again to turbulence, and the turbulent characteristics of forced convection appear.

In general, turbulent energy is mainly produced through mean shear motion. However, in the combined-convection boundary layer, the intensity of velocity fluctuation decreases in spite of the mean velocity gradient larger than that in turbulent pure natural convection as shown in Fig. 3. It has been found that the near-wall turbulence structure of natural convection significantly differs from those of forced convection (Tsuji et al., 1992). The occurrence of laminarization and peculiar intensity profile of velocity fluctuation with the addition of freestream velocity will also reveal the inherent difference between the structures of natural and forced convection.

The changes in the intensity of temperature fluctuation t with the transition from turbulence to laminar are shown in Fig. 6, being normalized by the temperature difference between the surface temperature T_w and the ambient temperature T_∞. The intensity of temperature fluctuation varies rapidly with the increase in freestream velocity, keeping step with the change in the velocity fluctuation intensity. The increasing and decreasing tendencies of the maximum intensity of temperature fluctuation have a close resemblance to those of velocity fluctuation. At $Grx/Rex^3 = 4.68 \times 10^{-4}$, the intensity profile of temperature fluctuation shows no great difference from that in pure natural convection. However, with increasing Grx/Rex^3, the temperature fluctuation intensity decreases, and the location of the maximum intensity gradually approaches the maximum mean velocity location. At $Grx/Rex^3 = 3.75 \times 10^{-5}$, the intensity of temperature fluctuation as well as that of velocity fluctuation becomes extremely small. Thus, the two-peak profiles did not appear in the temperature fluctuation intensity.

Fig. 7 shows the streamwise turbulent heat flux $\overline{ut}$ normalized by the maximum mean velocity and the temperature difference. The turbulent heat flux in the natural-convection boundary layer shows a positive peak at the maximum mean velocity location and takes small negative values near the wall. With the addition of freestream velocity ($Grx/Rex^3 = 4.68 \times 10^{-4}$), $\overline{ut}$ decreases at the maximum mean velocity location and increases in the negative value near the wall. The value of Nux, however, remains that of pure natural convection. At $Grx/Rex^3 = 1.65 \times 10^{-4}$, the value of $\overline{ut}$ increases again at the maximum mean velocity location, whereas the negative value of $\overline{ut}$ decreases near the wall. Then, the value of Nux becomes larger than that in turbulent pure natural convection as seen in Fig. 2. With a further increase in freestream velocity ($Grx/Rex^3 = 1.05 \times 10^{-4}$), the profile of turbulent heat flux takes a zero crossing at the maximum mean velocity location from negative values near the wall to positive values. At $Grx/Rex^3 = 3.75 \times 10^{-5}$, the $\overline{ut}$ value also becomes almost zero in the whole boundary layer region.

As mentioned above, turbulent quantities observed in the combined-convection boundary layer suddenly change with a slight increase in freestream velocity. It seems to be very difficult to correctly predict such a behavior of turbulent combined convection with existing turbulence models. Although the accumulation of experimental data for turbulent combined convection remains paramount, some improvement in turbulence models will be also required.

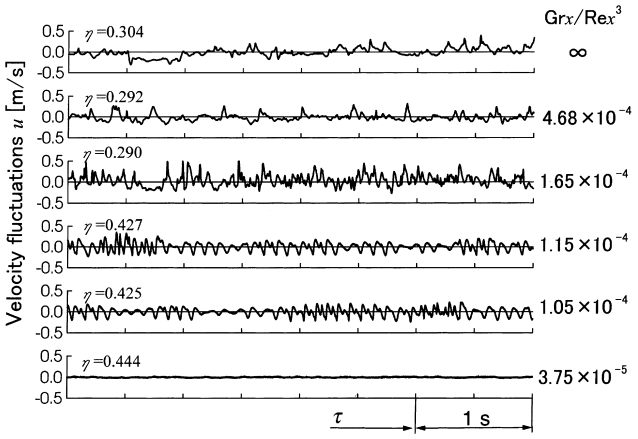

Fig. 8. Waveforms of velocity fluctuation.

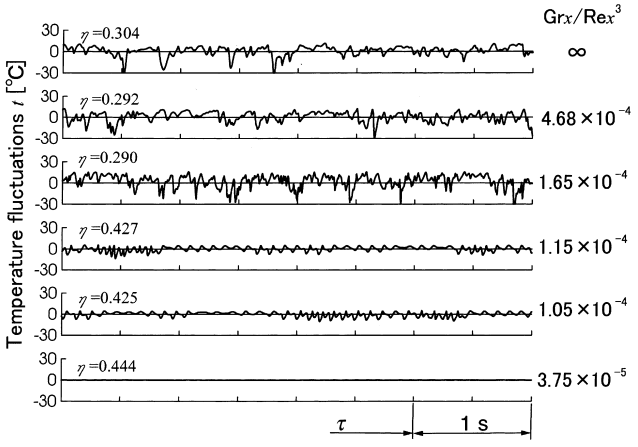

Fig. 9. Waveforms of temperature fluctuation.

3.4. Waveforms and spectra of velocity and temperature fluctuations

Waveforms of velocity fluctuation u and temperature fluctuation t measured at the near-wall location, where the mean velocity becomes about half the maximum mean velocity, are displayed in Figs. 8 and 9, respectively. In the case of turbulent pure natural convection, long-period waves indicating large-scale fluid motion are dominant in both the velocity and thermal fields. Though the waveforms at $Grx/Rex^3 = 4.68 \times 10^{-4}$ are still similar to those of pure natural convection, large-amplitude and high-frequency waveforms appear at $Grx/Rex^3 = 1.65 \times 10^{-4}$, which corresponds to the temporal increases in the intensities of velocity and temperature fluctuations near the wall as shown in Figs. 5 and 6. With a further increase in freestream velocity, the waveforms become smaller in amplitude, vary from random to harmonic with a specific frequency, and almost disappear at $Grx/Rex^3 = 3.75 \times 10^{-5}$.

Fig. 10 depicts the power spectra of velocity and temperature fluctuations, which are observed at the near-wall location where the mean velocity becomes about half the maximum mean velocity (solid line), at the maximum mean velocity location (broken line), and at the location in the outer region, where the mean velocity becomes the middle between the maximum and freestream velocities (dotted line), respectively. In the pure natural-convection boundary layer, fluctuations of several Hz are observed near the wall, and a large-scale fluid motion of a frequency lower than 1 Hz dominates in the outer

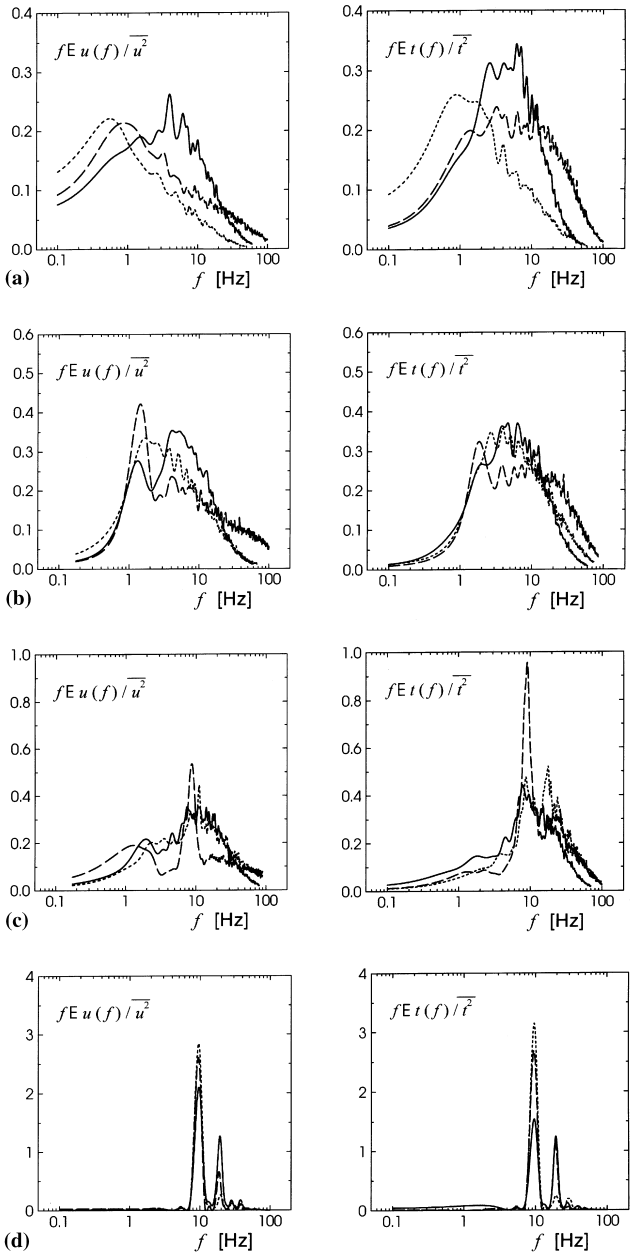

Fig. 10. Spectra of velocity and temperature fluctuations. *Solid line*: near wall location, *broken line*: maximum mean velocity location, *dotted line*: location in the outer region. (a) $Grx/Rex^3 = \infty$; (b) $Grx/Rex^3 = 4.68 \times 10^{-4}$; (c) $Grx/Rex^3 = 1.65 \times 10^{-4}$; (d) $Grx/Rex^3 = 1.05 \times 10^{-4}$.

region. With a slight addition of freestream, the scale of fluid motion begins to change. At $Grx/Rex^3 = 4.68 \times 10^{-4}$, the low frequency fluctuation suddenly decays, and the fluctuations in the frequency range of 1–10 Hz become evident over the whole boundary-layer region. As freestream velocity increases ($Grx/Rex^3 = 1.65 \times 10^{-4}$), the frequency of the most energetic fluctuation shifts toward the higher frequency region. Then, the spectrum at the maximum mean velocity location assembles at a specific frequency of 9 Hz. When laminarization is approached ($Grx/Rex^3 = 1.05 \times 10^{-4}$), spectrum peaks appear at the fundamental frequency of 9 Hz and its harmonic, which may imply that the linear fluid motions control the boundary layer.

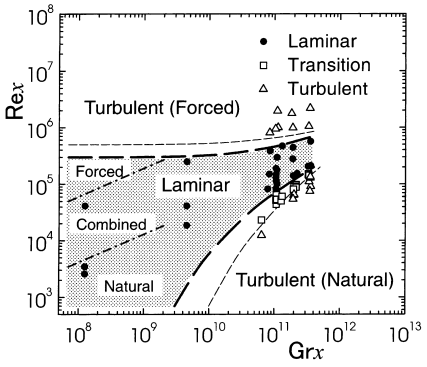

Fig. 11. Regimes of boundary layer flows.

3.5. Regimes of boundary layer flows

The classification of boundary layer flows is very important for engineering applications. Patel et al. (1998) proposed a map of the various convection flow regimes by utilizing the numerical results obtained with a low Reynolds-number k–ε turbulence model. Following their map, we have made a map based on the experiment. The boundary layer flows were identified in the following manner: when waveforms are random and the profiles of fluctuation intensities are similar to those in pure natural or pure forced convection, the flow regime is regarded as turbulence; in the case where harmonic waveforms with a specific frequency appear, the flow is regarded as transition; but the flow is regarded as laminar when the intensities of velocity and temperature fluctuations become almost zero and the profiles of mean velocity and mean temperature coincide with the theoretical ones obtained for the laminar combined-convection boundary layer.

The regimes of boundary layer flows in the coordinates $Re\,x$ and $Gr\,x$ are shown in Fig. 11. The transition regime corresponds to the region placed between the thick and thin dotted curves. For the laminar region, the flow regime can be identified as natural, combined and forced convection, based on the criterion that $Nu\,x$ deviates more than 5% from the calculated values for laminar pure natural and forced convections. This identification is shown with two chain lines (plotted as Richardson number $Rix = Grx/Rex^2 = 0.0276, 5.97$) in Fig. 11, which agree well with the result of Patel et al. (1998).

In the turbulent natural-convection boundary layer, the transition occurs at about $Grx = 3 \times 10^9$, and the turbulent boundary layer develops in the range $Grx > 10^{10}$. Nevertheless, with the addition of freestream velocity, the region of laminar combined convection extends to the large $Gr\,x$ region, and the transition is remarkably delayed: the boundary layer for $Rex \simeq 2 \times 10^5$ and $Grx \simeq 3 \times 10^{11}$ is still laminar, although the $Gr\,x$ value is 100 times as large as the critical Grashof number in pure natural convection. On the map presented by Patel et al. (1998), the region $Grx > 5 \times 10^9$ for moderate $Re\,x$ is divided into turbulent combined convection and turbulent natural convection. In practice, however, the laminar combined-convection regime appears in the region regarded as turbulent combined convection as shown in Fig. 11.

4. Conclusions

The fluid flow and heat transfer characteristics in the turbulent combined-convection boundary layer in air along a vertical heated plate were experimentally investigated with normal hot and cold wires, paying close attention to freestream conditions. The results of the present study may be summarized as follows:

1. A drastic reduction in $Nu\,x$ is observed in combined convection with a slight increase in freestream velocity, and the value of $Nu\,x$ decreases to about 40% of that in turbulent natural convection. This behavior of $Nu\,x$ is due to the boundary layer transition from turbulence to laminar, and the transition location is displaced in the region further downstream of that observed in pure natural convection. As the freestream velocity becomes sufficiently large, the boundary layer changes again to turbulence having the characteristics of forced convection
2. With a laminarization of the boundary layer, velocity and temperature fluctuations become smaller in amplitude and change from random to harmonic at a specific frequency, and an intensity profile having two peaks appears.
3. The regimes of boundary layer flows are classified based on the experimental results. With increasing freestream velocity, the region of laminar combined convection extends to the large $Gr\,x$ region far from the critical Grashof number in pure natural convection.

References

Carey, V.P., Gebhart, B., 1983. The stability and disturbance amplification characteristics of vertical mixed convection flow. J. Fluid Mech. 127, 185–201.

Fukatsu, R., 1934. Wind-Tunnel Experimental Method. Kyoritsusya, Tokyo (in Japanese).

Hall, W.B., Price, P.H., 1970. Mixed forced and free convection from a vertical heated plate to air. In: Proceedings of the Fourth International Heat Transfer Conference, vol. 4, NC 3.3.

Hattori, Y., Kashiwagi, E., Yamakawa, H., Wataru M., 1995. Experiments of natural convection to evaluate heat transfer in the spent fuel dry storage facilities. In: Proceedings of the Third International Conference on Nuclear Engineering, vol. 4, 1927–1932.

Hishida, M., Nagano, Y., 1978. Simultaneous measurements of velocity and temperature in nonisothermal flows. ASME J. Heat Transfer 100, 340–345.

Inagaki, T., Kitamura, K., 1988. Turbulent heat transfer of combined forced and natural convection along a vertical flat plate (effect of Prandtl number). JSME B 54, 2515–2522 (in Japanese).

Kitamura, K., Inagaki, T., 1987. Turbulent heat and momentum transfer of combined forced and natural convection along a vertical flat plate-aiding flow. Int. J. Heat Mass Transfer 30, 23–41.

Krishnamurthy, R., Gebhart, B., 1989. An experimental study of transition to turbulence in vertical mixed convection flows. ASME J. Heat Transfer 111, 121–130.

Lumley, J.L., 1964. Passage of a turbulent stream through honeycomb of large length-to-diameter ratio. ASME J. Basic Eng., 218–220.

Patel, K., Armaly, B.F., Chen, T.S., 1964. Transition from turbulent natural to turbulent forced convection. ASME J. Heat Transfer 120, 1086–1088.

Rae, W.H., Pope, A., 1984. A Low-speed Wind Tunnel Testing, second ed. Wiley, New York.

Tsuji, T., Nagano, Y., 1988. Characteristics of a turbulent natural convection boundary layer along a vertical flat plate. Int. J. Heat Mass Transfer 31, 1723–1734.

Tsuji, T., Nagano, Y., Tagawa, M., 1992. Experiment on spatio-temporal turbulent structures of a natural convection boundary layer. ASME J. Heat Transfer 114, 901–908.